Digital Communications and Networks (2015) 1, 171–180

HOSTED BY

ELSEVIER

Available online at www.sciencedirect.com

ScienceDirect

journal homepage: www.elsevier.com/locate/dcan

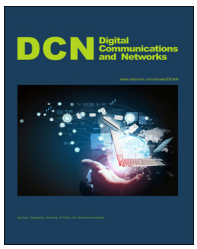

Optical power allocation for adaptive transmissions in wavelength-division multiplexing free space optical networks ☆

Hui Zhou[a,b], Shiwen Mao[a,*], Prathima Agrawal[a]

[a]Department of Electrical and Computer Engineering, Auburn University, Auburn, AL 36849-5201, USA
[b]Amazon Web Service, Amazon Inc., 345 Boren Ave N, Seattle, WA 98109, USA

Received 17 August 2015; accepted 5 September 2015
Available online 28 September 2015

KEYWORDS
Free space optics;
Radio over free space optics;
Wavelength-division multiplexing

Abstract
Attracting increasing attention in recent years, the Free Space Optics (FSO) technology has been recognized as a cost-effective wireless access technology for multi-Gigabit rate wireless networks. Radio on Free Space Optics (RoFSO) provides a new approach to support various bandwidth-intensive wireless services in an optical wireless link. In an RoFSO system using wavelength-division multiplexing (WDM), it is possible to concurrently transmit multiple data streams consisting of various wireless services at very high rate. In this paper, we investigate the problem of optical power allocation under power budget and eye safety constraints for adaptive WDM transmission in RoFSO networks. We develop power allocation schemes for adaptive WDM transmissions to combat the effect of weather turbulence on RoFSO links. Simulation results show that WDM RoFSO can support high data rates even over long distance or under bad weather conditions with an adequate system design.

1. Introduction

Recently, demand for multimedia service with high quality of service (QoS) requirements has been drastically increasing. To cater to the increasing demand on capacity, optical fibers have been utilized for years to deliver high volume of data, often between central and remote universal stations. Due to the relatively high cost of deploying optical fibers, Free Space Optics (FSO) has been developed as a cost-effective alternative wireless access technology for multi-Gigabit rate communication networks. FSO provides an excellent alternative to optical fiber systems for last-mile access networks [1], ranging from local area network (LAN)-to-LAN connection for enterprise/campus, high capacity military communications, to disaster recovery and emergency response, among others.

☆This work was presented in part at the 2014 IEEE Wireless Communications and Networking Conference (WCNC), Istanbul, Turkey, April 2014.

*Corresponding author.
E-mail addresses: hzz0016@tigermail.auburn.edu (H. Zhou), smao@ieee.org (S. Mao), agrawpr@auburn.edu (P. Agrawal).

http://dx.doi.org/10.1016/j.dcan.2015.09.001

Attracting considerable attention from the research community, the FSO technology has also been developed for carrying various wireless services, as known as Radio on Free Space Optics (RoFSO). FSO systems can operate on wavelengths in the 1520–1600 nm range, which makes the development of wavelength-division multiplexing (WDM) RoFSO systems feasible. Advanced Dense Wavelength Division Multiplexing (DWDM) RoFSO systems have been developed to support the simultaneous transmission of multiple wireless signals [1]. Despite of its great potential of supporting data intensive communications for various applications, a line-of-sight (LOS) path is required in any FSO system. Consequently, FSO is highly susceptible to the atmospheric environment due to the inhomogeneity of air temperature and pressure, or flying objects [2]. To harvest the high potential of RoFSO, fading-mitigation techniques should be employed to mitigate atmospheric turbulence-induced intensity fluctuations.

To this end, topology control [3,2,4,5], load-balancing [6], and spatial diversity techniques [7] have been studied and proved to be effective in maintaining a good system performance. Adaptive transmissions have been recently introduced into FSO systems and is emerging as a potential solution to mitigate the effect of atmospheric turbulence [8]. In FSO systems, channels are usually slow-fading and FSO transceivers have full-duplex capabilities. With negligible effect on data rates, a small portion of the bandwidth can be used for feedback of channel state information (CSI). In some hybrid RF/FSO systems, the RF channel can be used for CSI feedback [9]. Thus reliable CSI could be available in FSO systems, which will be highly useful for designing adaptive transmission schemes.

In this paper, we propose optical power allocation schemes for an adaptive WDM RoFSO system in which variable wavelengths are adopted to mitigate the effect of weather turbulence [10]. Proposed optical power allocation schemes optimally allocate transmit power to achieve maximum capacity and enhance the performance of the WDM RoFSO system. Nowadays, the bandwith wavelengths between 1520 nm and 1600 nm have already been used in FSO systems. Furthermore, the emerging quantum cascade laser (QCL) technology can offer great flexibility on adjusting an RoFSO transceiver to operate on the optimal transmit wavelengths [11]. Under a total power constraint, different optical powers can be allocated to the chosen wavelengths in a WDM RoFSO system, to achieve further enhanced system performance.

We investigate the problem of optical power allocation under the total power budget and eye safety power constraints for adaptive WDM transmission in RoFSO systems. To achieve capacity gain, we first analyze a conventional FSO system and develop a simple water-filling based algorithm to derive the optimal power allocation for the chosen wavelengths. For WDM RoFSO systems, a near-optimal RoFSO power allocation algorithm is developed based on the reformulation-linearization technique (RLT) [12], which can provide a linear programming (LP) relaxation of the complex problem. A computationally efficient scheme is also developed based on an approximation of the channel model. Finally, we investigate the diversity gain in the WDM RoFSO system. The performance of the proposed schemes is evaluated with simulations, and is demonstrated to be highly effective for achieving high system capacity under various scenarios.

The remainder of this paper is organized as follows. The related work is discussed in Section 2. The system model is presented in Section 3, while the three power allocation schemes are developed in Section 4 to fully utilize DWDM RoFSO systems. Simulation results are analyzed in Section 5. Section 6 concludes this paper.

2. Related work

Attracting significant interest both in academia and industry, the FSO technology has been recognized as a promising solution for high capacity, long distance communications. The performance of FSO networks is highly depend on the availability and reliability of the LOS path since an FSO transmitter is highly directional. Weather turbulence strongly affects FSO communication links. Weather effects on the connectivity of FSO networks were studied in [13]. The influence of turbulence-accentuated interchannel crosstalk on WDM FSO system performance has been studied in [14].

Many fading-mitigation techniques have recently been employed to maintain a good FSO system performance. In [15], a multipath fading resistant FSO communication system architecture was introduced to combat adverse weather conditions. Spatial diversity techniques, extensively studied in conventional RF communication systems [16], can also be applied in FSO systems to improve system performance. A multiple-input multiple-output (MIMO) FSO system can achieve significant diversity gain in the presence of atmospheric fading by deploying multiple transmit or receiver apertures [7,17]. A cooperative diversity technique [18–20] is also a cost-effective alternative to maintain system performance. In a recent work [21], a one-relay cooperative diversity scheme was proposed for combating turbulence-induced fading, while cooperative diversity was analyzed for non-coherent FSO communications.

Adaptive transmission technology has been introduced into FSO systems to mitigate weather turbulence. Djordjevic in [22] applied the conventional wireless adaptive modulation and coding method in an FSO system and further studied adaptive low-density-parity-check (LDPC) coded modulation to compensate performance degradation when turbulence is strong. Karimi and Uysal in [8] designed transmission algorithms with consideration of the number of bits carried per chip time (BpC) in an FSO link, in which intensity modulation/direct detection (IM/DD) with M-ary pulse position modulation (M-PPM) was employed. Several other adaptive schemes have also been proposed and studied. In [11], the authors proposed using variable wavelength to combat the effects of atmospheric interference. Varying wavelength becomes feasible as the QCL technology becomes more mature. In [23], the authors proposed an adaptive transmission scheme to satisfy the requirements of various wireless services. A WDM power allocation method considering Optical Modulation Index (OMI) was proposed in their adaptive RoFSO system design. The authors in [24] studied the potential of the MIMO channel for combating link fading. However, the performance of the FSO MIMO system is constrained by the

thermal noise limited receivers and thus Avalanche photodiodes (APDs) [25] were studied and commonly used in FSO systems.

In this paper, we propose power allocation schemes for adaptive WDM transmissions to achieve capacity gain or diversity gain. WDM has been employed in FSO transmission systems and has been shown to be capable of supporting very high data rate transmission in [26]. RoFSO technology makes it possible to transmit multiple RF signals using WDM. RoFSO provides a promising alternative to optical fiber systems. In [27], the authors designed and evaluated an RoFSO system as an universal platform for the integration of optical fiber and FSO networks. In [28], optical fading in FSO Channels was statistically analyzed, while [1] provides a comprehensive study of RoFSO and the satisfactory results confirmed that the effect of scintillation on RoFSO performance can be estimated by an analytical model.

In the adaptive WDM RoFSO system we studied, a variable number of wavelengths are adopted to mitigate weather turbulence and optical transmit power is optimally allocated to achieve maximum capacity gain. Although turbulence may not change significantly with wavelength in some weather conditions, considering the huge bandwidth that the DWDM RoFSO system can support, it is still non-trivial to study the problem of utilizing wavelength properly. Moreover, since QCL technology can offer great flexibility on adjusting wavelengths, more wavelengths can be utilized as FSO systems advance. Alternatively, the multiple wavelengths used in the WDM RoFSO system can be utilized to achieve robustness of the system.

Table 1 Table of notation.

Symbol	*Definition*
h_l	FSO link attenuation
h_f	Atmospheric turbulence
A_{TX}	Aperture area of the transmitter
A_{RX}	Aperture area of the receiver
α	Atmospheric attenuation coefficient
V	Visibility in kilometers
Λ	Wavelength
q	A parameter related to visibility
CNR	Carrier to noise ratio
OMI	Optical modulation index
RIN	Relative intensity noise
K	Boltzman's constant
T	Temperature
m	Photodiode gain
e	Electrical charge
F	Excess noise factor
G_f	Photodiode output conductance
h	Channel state of a FSO link
B	Bandwidth
N	Number of available wavelength bands
M	Number of used wavelength bands
h_i	Channel gain for channel i
P_i	Optical power allocated to channel i
$\overline{P}$	Peak power bound for transmitted pulse
P_{max}	Power budget
λ, λ_i	Lagrange multipliers

3. System and channel model

In this section, we will introduce the channel model and system models. We summarize the notation used in this paper in Table 1.

3.1. Channel model

FSO transceivers are highly directional, but FSO links are prone to degradation due to weather turbulence. We consider both effects of path loss and turbulence-induced fading over FSO links [18]. The optical channel state h is modeled as a product of two factors

$$h = h_l \cdot h_f, \tag{1}$$

where h_l denotes the attenuation and h_f represents the atmospheric turbulence. Attenuation h_l is a function of optical wavelength Λ and link distance d, as

$$h_l = \frac{A_{TX}A_{RX} \cdot e^{-\alpha d}}{(\Lambda \cdot d)^2}, \tag{2}$$

where A_{TX} and A_{RX} are the aperture areas of transmitter and receiver, respectively. The atmospheric attenuation coefficient α is given by

$$\alpha = \left(\frac{3.91}{V}\right) \cdot \left(\frac{\Lambda}{55}\right)^{-q}, \tag{3}$$

where V is the visibility in kilometers and q is a parameter related to the visibility as [8]

$$q = \begin{cases} 0.585V^{1/3}, & V \le 6 \text{ km} \\ 1.3, & 6 \text{ km} \le V \le 50 \text{ km}. \end{cases} \tag{4}$$

For fading h_f, we assume atmospheric turbulence can be modeled as a log-normal distribution [29]. The log-normal model is a widely used fading model, especially under weak-to-moderate turbulence conditions.

The channel model for an FSO link can be written as

$$y = h \cdot P_t \cdot x + n, \tag{5}$$

where x and y are transmitted and received signal respectively; P_t is the power of the transmitted pulse; and n is the additive Gaussian noise.

3.2. System model

RoFSO is a new technology that provides high data rate and reliable transmission. The RoFSO system using WDM allows simultaneous transmission of multiple data streams consisting of various wireless and wireline services at very high rates. An advanced DWDM RoFSO system is illustrated in Fig. 1 [1].

We assume a WDM FSO system that is capable of operating in the wavelength band from 1520 nm to 1600 nm. Apart from the data-transmitting antenna, we assume that an atmospheric influence measurement antenna or weather measurement device is equipped at the FSO BS. Thus, we can estimate atmospheric loss for channels using different

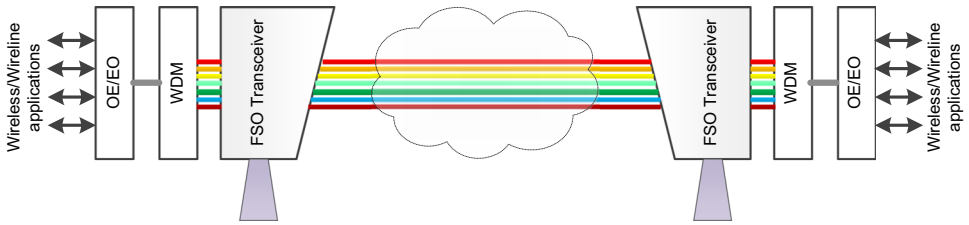

Fig. 1 Illustration of an advanced DWDM RoFSO system.

wavelengths. Alternatively, CSI can be obtained by using a small portion of the bandwidth to provide channel information without tangibly affecting the data rate. In some hybrid RF/FSO systems, the RF channel can be used for CSI feedback. Since atmospheric turbulence is a major degrading factor in FSO systems, we propose power allocation schemes for the adaptive RoFSO system, in which both wavelength and transmit power will be adaptively allocated according to channel conditions.

An important parameter to evaluate the performance of RF-FSO is the carrier to noise ratio (CNR). The CNR of an RoFSO system using an APD photo detector is given as [1]

$$\mathrm{CNR} = \frac{0.5(\mathrm{OMI}\cdot mP_r)^2}{\mathrm{RIN}\cdot P_r^2 + 2em^{(2+F)}P_r + 4KT\cdot G_f}, \tag{6}$$

where OMI is the optical modulation index, m is the photodiode gain, T is the temperature, K is Boltzman's constant, e is the electrical charge and G_f is the photodiode output conductance. In the denominator, $4\,KTG_f$ is thermal noise; F is the excess noise factor; m is the photodiode gain; e is the electrical charge; $2em^{(2+F)}P_r$ is the optical short noise; and $RINP_r^2$ is the relative intensity noise from Laser diode (LD). The numerator represents the received signal power. $P_r = rP_{pd}$, where r is the photodiode responsivity and P_{pd} is the received power at the detector and is given as the product of transmit power and channel gain. Without loss of generality, we assume all tones are modulated with the same OMI that will not introduce intermodulation distortion.

4. Adaptive WDM transmission

To mitigate the effect of weather turbulence, we adapt wavelength and adjust power allocation to achieve better system performance. First, we consider an RoFSO system using wavelength Λ in the range of [1520,1600] nm. The available wavelengths are divided into N parts, which are non-overlapping with adequate spacing. We assume the FSO channel is slow varying [8]. For each channel with wavelength Λ_i, we can estimate its channel state h_i or obtain the channel state through a feedback channel.

In different weather conditions, it is desirable to choose the wavelengths that have the best channel conditions. We assume that the WDM FSO system will use at most M different wavelengths. Among the N available wavelengths, we will first choose M wavelengths that have the greatest channel gains. The next step is to allocate transmit powers to different wavelengths such that the system capacity is maximized.

4.1. Conventional FSO system

We first consider conventional modeling of wireless channels under white Gaussian noise. For the sake of simplicity, we define channel gain over noise for channel i by abusing of notation as

$$h_i = \frac{|h_l \cdot h_f|^2}{N_0}. \tag{7}$$

According to the estimated channel gains, we choose M wavelengths that can offer the greatest channel gains from the N available wavelengths. Here M is a constant jointly determined by the channel conditions and the capacity need of the system. It can be set to N, for example, if all the wavelengths are to be used.

Let P_i be the optical power allocated to channel i. Due to fixed power budget P_{max} for each FSO base station, we have the following total power constraint:

$$\sum_{i=1}^{M} P_i \le P_{max}. \tag{8}$$

In FSO systems, eye safety should always be taken into consideration in the system design. Thus we have the additional power constraint

$$0 \le P_i \le \overline{P} \quad \text{for all } i. \tag{9}$$

where $\overline{P}$ is the peak power bound for the transmit powers. Thus, we formulate the following capacity maximization problem:

$$\max \quad \sum_{i=1}^{M} \log(1 + P_i \cdot h_i) \tag{10}$$

$$\text{s.t.} \quad \sum_{i=1}^{M} P_i \le P_{max} \tag{11}$$

$$0 \le P_i \le \overline{P}, \ \text{for all } i. \tag{12}$$

By applying Karush-Kuhn-Tucker (KKT) theorem, we can find that optimal power allocation satisfies

$$\begin{cases} P_i = \min\left\{\overline{P}, \left[\frac{1}{\lambda} - \frac{1}{h_i}\right]^+\right\} \\ \sum_{i=1}^{M} P_i = P_{max}, \end{cases} \tag{13}$$

where λ is the Lagrange multiplier. The inverse of λ is often regarded as the water level.

The algorithm to solve the capacity maximization problem is to first sort the channels according to their channel gains. We then find the number of channels n, which are

allocated with a nonzero power, as in Steps 2–3. The water volume H_n that is required to fill n channels can be calculated as

$$\sum_{i=1}^{n} i \cdot \left(\frac{1}{h_{i+1}} - \frac{1}{h_i}\right),$$

and H_n should not be greater than P_{max}. Then we can calculate the water level and allocate power to each selected channel according to (13). This procedure is based on the assumption that a feasible power should also satisfy the eye safety power constraint. If the allocated power $(1/\lambda - 1/h_i)$ is greater than $\overline{P}$, we need to adjust the water level accordingly. The detailed water-filling algorithm is presented in Algorithm 1.

Algorithm 1. The water-filling algorithm.

1 Sort channels according to channel gains as: $h_1 \geq h_2 \geq \ldots \geq h_M$;
2 Calculate $H_n = \sum_{i=1}^{n} i(1/h_{i+1} - 1/h_i)$;
3 Find n such that $H_{n+1} \geq P_{max} \geq H_n$;
4 Determine Water level: $(1/\lambda) = (1/n)(P_{max} + \sum_{i=1}^{n}(1/h_i))$;
5 Allocate power to each channel: $P_i = [1/\lambda - 1/h_i]^+$, for all i ;
6 **if** $P_i \leq \bar{P}$, *for all* i **then**
7 | Terminate with the power allocation ;
8 **end**
9 Set $i = 1$;
10 **while** $P_i > \bar{P}$ **do**
11 | Set $P_i = \bar{P}$ and $P_{max} = P_{max} - \bar{P}$;
12 | Delete channel i in the next power allocation round ;
13 | i++ ;
14 **end**
15 Go to Step 2 ;

4.2. DWDM RoFSO system

Next, we develop the model for the RoFSO channels as described in Section 3, which is more suitable for RoFSO using APD photo-detectors. CNR defined in Section 3.2 will be an important parameter to evaluate the RoFSO performance.

4.2.1. Reformulation and relaxation based approach

To simplify notation, we denote the constant $0.5(m\text{OMI})^2$ by a, the relative intensity noise level RIN by b, the optical short noise $2em^{(2+F)}$ by c, and the thermal noise $4KTG_f$ by d. Thus, our adaptive power allocation problem becomes

$$\max \quad \sum_{i=1}^{M} \log\left(1 + \frac{a_i(P_i h_i)^2}{b_i(P_i h_i)^2 + c_i P_i h_i + d_i}\right) \tag{14}$$

$$\text{s.t.} \quad \sum_{i=1}^{M} P_i \leq P_{max} \tag{15}$$

$$0 \leq P_i \leq \overline{P} \quad \text{for all } i. \tag{16}$$

If we denote CNR by

$$\gamma_i = \frac{a_i(P_i h_i)^2}{b_i(P_i h_i)^2 + c_i P_i h_i + d_i}, \tag{17}$$

the optimization problem, termed Problem OPT-RoFSO, can be rewritten as

$$\max \quad \sum_{i=1}^{M} \log(1+\gamma_i) \tag{18}$$

$$\text{s.t} \quad \sum_{i=1}^{M} P_i \leq P_{max} \tag{19}$$

$$0 \leq P_i \leq \overline{P} \quad \text{for all } i \tag{20}$$

$$\gamma_i = \frac{a_i(P_i h_i)^2}{b_i(P_i h_i)^2 + c_i P_i h_i + d_i} \quad \text{for all } i. \tag{21}$$

It is challenging to solve this problem due to its complexity and nonlinear nonconvex properties. In the following, we adopt the RLT technique to obtain an LP relaxation of Problem OPT-RoFSO and derive a feasible near-optimal solution [12].

The RLT relaxation is as follows. Letting

$$c_i = \log(1+\gamma_i),$$

the objective function $\sum_{i=1}^{M} c_i$ will now be linear and new constraints $c_i = \log(1+\gamma_i)$ are introduced. We first linearize the logarithmic terms in the new constraints using the polyhedral outer approximation as follows.

From (21), it can be seen that γ_i is a monotone increasing function of P_i. Letting P_i be 0 and $\overline{P}$, we obtain the lower and upper bounds of γ_i, respectively. We denote the upper bound of γ_i by $\overline{\gamma}_i$, while the lower bound is 0. We use the four-point approximation and obtain the following new linear constraints:

$$\begin{cases} c_i \geq \dfrac{\gamma_i}{\overline{\gamma}_i} \cdot \log(1+\overline{\gamma}_i) \\ c_i \leq \log(1+\gamma_i^k) + \dfrac{\gamma_i - \gamma_i^k}{1+\gamma_i^k}, \end{cases} \tag{22}$$

where

$$\gamma_i^k = \frac{1}{3} \cdot k\overline{\gamma}_i \quad \text{for } k = 0, 1, 2, 3.$$

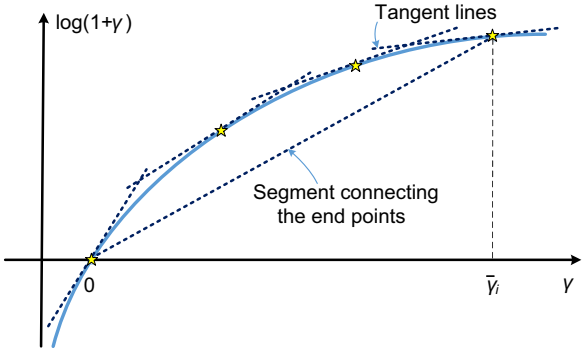

Fig. 2 Four-point polyhedral outer approximation for $\log(1+\gamma)$.

The first equation in (22) is for the segment connecting the two end points of the logarithm function and the second equation in (22) is for the tangent lines at the four points on the logarithm function respectively. A four-point approximation for $\log(1+\gamma)$ is illustrated in Fig. 2. The corresponding convex envelope is formed by four tangent lines and a chord connecting the two end points.

Problem OPT-RoFSO now becomes a polynomial programming problem. We next introduce substitution variables and the corresponding RLT bound-factor product constraints to remove the quadratic terms and to obtain an LP relaxation. Specifically, constraint (21) contains quadratic terms. We can rewrite (21) as

$$b_i(P_i h_i)^2\gamma_i + c_i h_i P_i \gamma_i + d_i\gamma_i - a_i(P_i h_i)^2 = 0. \tag{23}$$

To remove quadratic terms, we define substitution variables

$$\begin{cases} u_i = P_i^2 \text{ for all } i \\ v_i = \gamma_i P_i \text{ for all } i \\ w_i = \gamma_i u_i \text{ for all } i \\ \beta_i = c_i v_i \text{ for all } i. \end{cases} \tag{24}$$

Thus constraint (21) becomes

$$b_i h_i^2 w_i + h_i\beta_i + d_i\gamma_i - a_i h_i^2 u_i = 0. \tag{25}$$

Since P_i is bounded, it can easily show that $u_i \in (0, \overline{P}^2)$. For variables v_i, with $0 \le \gamma_i \le \overline{\gamma}_i$ and $0 \le P_i \le \overline{P}$, we can obtain the following RLT bound-factor product constraints:

$$\begin{cases} (\gamma_i - 0)(P_i - 0) \ge 0 \\ (\overline{\gamma}_i - \gamma_i)(P_i - 0) \ge 0 \\ (\gamma_i - 0)(\overline{P} - P_i) \ge 0 \\ (\overline{\gamma}_i - \gamma_i)(\overline{P} - P_i) \ge 0. \end{cases} \tag{26}$$

Substituting $v_i = \gamma_i P_i$, we obtain the following four linear constraints for variable v_i:

$$\begin{cases} v_i \ge 0 \\ \overline{\gamma}_i P_i - v_i \ge 0 \\ \overline{P}\gamma_i - v_i \ge 0 \\ \overline{P}\overline{\gamma}_i - \overline{\gamma}_i P_i - \overline{P}\gamma_i + v_i \ge 0. \end{cases} \tag{27}$$

For variable w_i, with $0 \le \gamma_i \le \overline{\gamma}_i$ and $0 \le u_i \le \overline{P}^2$, we obtain the following four linear constraints in the same manner:

$$\begin{cases} w_i \ge 0 \\ \overline{\gamma}_i u_i - w_i \ge 0 \\ \overline{P}^2\gamma_i - w_i \ge 0 \\ \overline{P}^2\overline{\gamma}_i - \overline{\gamma}_i u_i - \overline{P}^2\gamma_i + w_i \ge 0. \end{cases} \tag{28}$$

We deal with the variables β_i in the same manner, with $0 \le c_i \le \overline{c}_i$ and $0 \le v_i \le \overline{\gamma}_i\overline{P}$, and obtain the following four linear constraints for variable β_i.

$$\begin{cases} \beta_i \ge 0 \\ \overline{c}_i v_i - \beta_i \ge 0 \\ \overline{\gamma}_i\overline{P}c_i - \beta_i \ge 0 \\ \overline{c}_i\overline{\gamma}_i\overline{P} - \overline{\gamma}_i\overline{P}c_i - \overline{c}_i v_i + \beta_i \ge 0, \end{cases} \tag{29}$$

where $\overline{c}_i = \log(1+\overline{\gamma}_i)$.

Now the original problem is relaxed to an LP problem with the additional constraints and variables as follows:

$$\max \quad \sum_{i=1}^{M} c_i \tag{30}$$

$$\text{s.t.} \quad \sum_{i=1}^{M} P_i \le P_{max} \tag{31}$$

$$0 \le P_i \le \overline{P} \quad \text{for all } i \tag{32}$$

$$0 \le u_i \le \overline{P}^2 \quad \text{for all } i \tag{33}$$

$$b_i h_i^2 w_i + h_i\beta_i + d_i\gamma_i - a_i h_i^2 u_i = 0, \quad \text{for all } i \tag{34}$$

$$\text{New linear constraints (22) forall } i \tag{35}$$

$$\text{RLT bound} - \text{factor constraints (27), (28) and (29) for all } i. \tag{36}$$

The relaxed problem can be solved in polynomial time with an LP solver. Note that during the procedure of reformulation and linearization, we preserve the original power constraints of Problem OPT-RoFSO, i.e., (19) and (20). Hence the optimal transmit power allocation policy obtained for the LP relaxation is also feasible to the original problem OPT-RoFSO. The feasibility of the LP solution is summarized in the following proposition:

Proposition 1. *The optimal transmit power allocation policy to the LP relaxation of Problem OPT-RoFSO is a feasible solution to the original problem.*

4.2.2. A faster near-optimal algorithm

Due to the complexity of the RLT-based method, it may not be suitable when the channels vary quickly. We next develop a more computationally cost-effective scheme in the following. If we ignore the relative intensity noise and optical short noise, CNR can be approximated by $0.5P_r^2(m\text{OMI})^2/4KTG_f$. To simplify notation, we denote constant value $0.5(m\text{OMI})^2/4KTG_f$ by a. We obtain the following optimization problem:

$$\max \quad \sum_{i=1}^{M} \log\left(1 + a_i(P_i h_i)^2\right) \tag{37}$$

$$\text{s.t.} \quad \sum_{i=1}^{M} P_i \le P_{max} \tag{38}$$

$$0 \le P_i \le \overline{P} \quad \text{for all } i. \tag{39}$$

According to Karush-Kuhn-Tucker (KKT) theorem, if $\boldsymbol{P}^\star = [P_1^\star, P_2^\star, \cdots, P_M^\star]$ is a local maximizer for the above optimization problem, there exists $\lambda \in \mathbb{R}$ and $\lambda_i \in \mathbb{R}$, for

$i \in \{1, 2, \cdots, M\}$, such that

$$\begin{cases} \frac{\partial[\log(1+a_i(P_i^\star h_i)^2)]}{\partial P_i} - \lambda - \lambda_i = 0 \quad \text{for all } i \\ \lambda\left(\sum_{i=1}^{M} P_i^\star - P_{max}\right) = 0 \\ \lambda_i(P_i^\star - \overline{P}) = 0 \quad \text{for all } i \\ \lambda \geq 0, \\ \lambda_i \geq 0 \quad \text{for all } i. \end{cases} \tag{40}$$

According to (40), if $\lambda_i > 0$, then $P_i^\star = \overline{P}$; and if $\lambda_i = 0$, we can solve (40) to have

$$P_i^\star = \frac{1}{\lambda} + \sqrt{\frac{1}{\lambda^2} - \frac{1}{a_i h_i^2}}. \tag{41}$$

Thus we find that the optimal power allocation satisfies

$$\begin{cases} P_i = \min\left\{\overline{P}, \frac{1}{\lambda} + \sqrt{\frac{1}{\lambda^2} - \frac{1}{a_i h_i^2}}\right\}, \quad \text{if } \lambda^2 \lambda a_i h_i^2 \\ P_i = 0, \text{otherwise} \\ \sum_{i=1}^{M} P_i = P_{\max}. \end{cases} \tag{42}$$

Regarding the inverse of λ as some kind of "water level," we find that the greater the channel gain, the larger the deviation of the power allocated to this channel from the water level. Usually we cannot directly solve from (42) for the optimal power allocation. An iterative algorithm is needed to obtain an appropriate λ and solve this optimization problem. The detailed algorithm is presented in Algorithm 2.

Algorithm 2. RoFSO power allocation algorithm.

```
Sort channels according to channel gains as:
h_1 ≥ h_2 ≥ ... ≥ h_M ;
Solve Σ_{i=1}^{M} P_i = P_max numerically according to (42) ;
Obtain λ and calculate P_i for i ∈ [1, M] according
to (41) ;
if P_i ≤ P̄, for all i then
    Terminate with the power allocation ;
end
Set i = 1 ;
while P_i > P̄ do
    Set P_i = P̄ ;
    i++ ;
end
Go to Step 2 ;
```

5. Performance evaluation

In this section, we evaluate the performance of the proposed algorithms with MATLAB simulations. We calculate channel gains as shown in Section 3.1 and CNR are calculated according to (6) for the evaluated schemes. The simulation parameters are the same from prior work and are listed in Table 2 [1,23].

We investigate the three algorithms introduced in the previous section for power allocation in the WDM RoFSO system. Wavelengths in the band 1520-1580 nm are assumed in our WDM RoFSO simulations. We adopt a 5 nm spacing between adjacent wavelengths used in the simulations.

In Fig. 3, we compare the three algorithms introduced in Section 4 and examine the impact of the power budget on the total system capacity. We increase P_{max} from 0.5 to 1 with step-size 0.1 and plot the total capacity. As can be seen in Fig. 3, the RoFSO power allocation algorithm outperforms the other two algorithms with considerable gains. Since the relative intensity noise and the optical short noise are very small in our simulations, the RoFSO power allocation algorithm will achieve the best near-optimal solution. The RLT algorithm, although consumes much running time, can only produce an optimal power allocation for the relaxed LP problem. The power allocation solution obtained from RLT is feasible but achieves the worst performance in terms of capacity gain due to relaxation. We also find that the total capacity increases along with the power budget for both the water-filling algorithm and RoFSO power allocation algorithm, albeit not obviously for the latter. After the power budget becomes even larger, there is much less space for capacity increment due to the eye safety power constraint.

Next, we examine the effect of weather conditions on the system capacity in Fig. 4. The distance between FSO BS's is set to 500 m. We change the weather condition from clear to foggy by changing the atmospheric attention coefficient. The coefficient is 0.48 db/km for clear weather, 2.8 db/km

Table 2 Simulation parameters.

Symbol	*Value*	*Definition*
D_t	15 mm	Tx. aperture diameter
D_r	0.1 m	Rx. aperture diameter
B	1 GHz	Bandwidth
d	1 km	Distance
P_{max}	0.5 W	Power budget
$\overline{P}$	0.1 W	Peak power constraint
OMI	17.5%	Optical modulation index
m	5	Photodiode gain
RIN	−150 dB/Hz	Relatively intensity noise

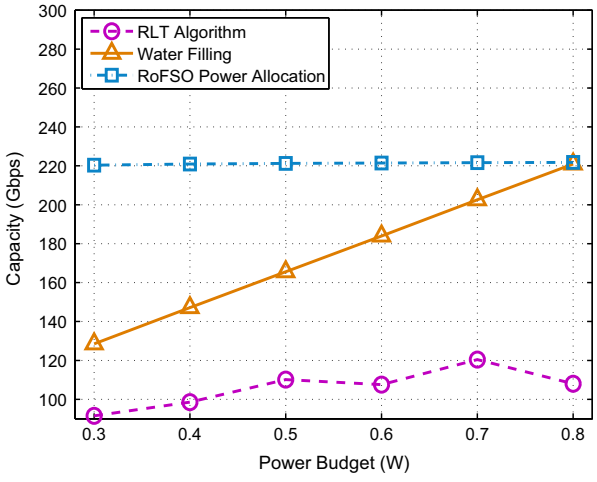

Fig. 3 System capacity versus the power budget P_{max}.

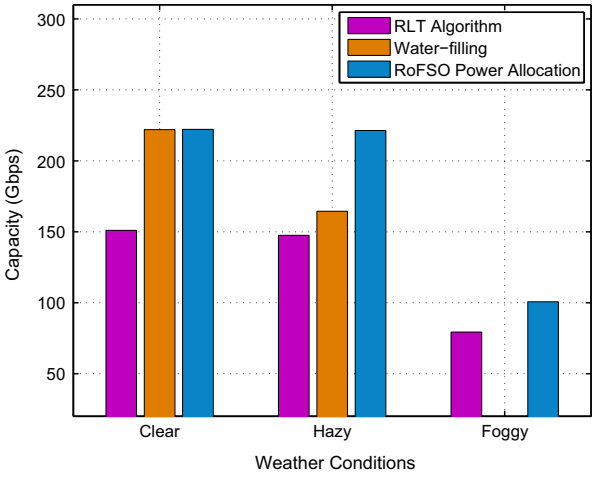

Fig. 4 System capacity versus weather condition.

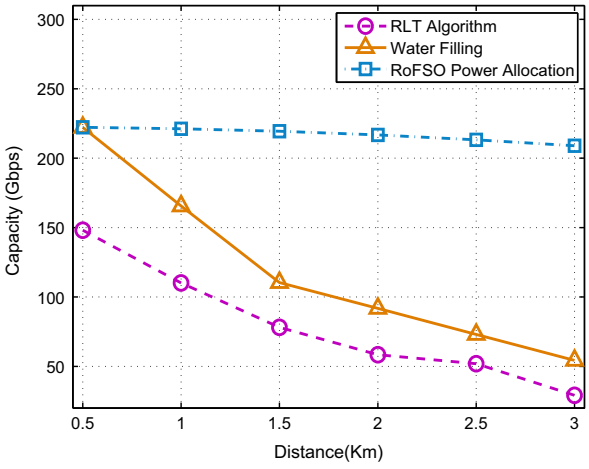

Fig. 5 System capacity versus distance.

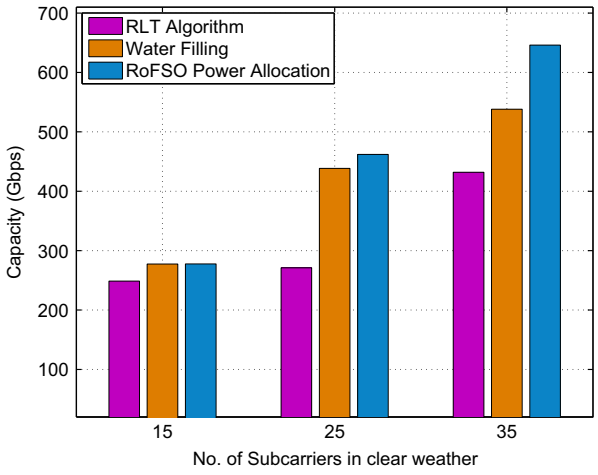

Fig. 6 System capacity versus the number of subcarriers in clear weather.

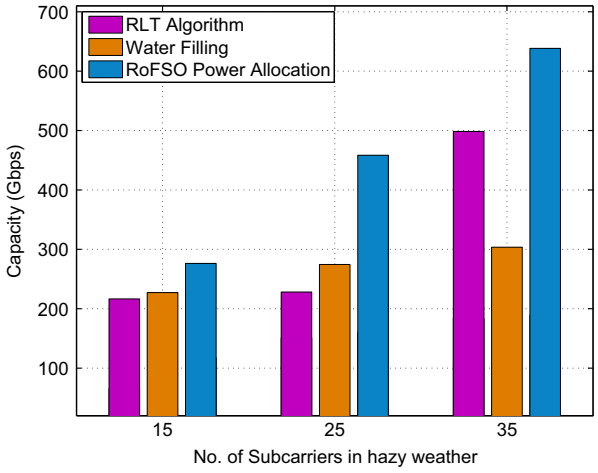

Fig. 7 System capacity versus the number of subcarriers in hazy weather.

for hazy weather, and 15 db/km for foggy weather [30]. As can be seen from Fig. 4, the system capacity decreases as weather gets worse. We also find that the simple water-filling algorithm which is developed for conventional RF systems is not suitable for the RoFSO system when weather condition is severe. The capacity achieved by the simple water-filling algorithm decrease the most as the weather becomes worse. When the weather is foggy, the capacity achieved by the water-filling algorithm is about 10 Gbps.

We also plot the total capacity vs. the distance between the FSO BS's in Fig. 5. As expected, the total capacity decreases as the distance is increased. When the distance between the FSO transceivers is relatively small, the difference between the capacities achieved by three algorithms is also small. But as we increase the distance from 500 m to 1 km or even greater, the capacities achieved by simple water filling algorithm and RLT algorithm drop dramatically. The capacity obtained by using the RoFSO power allocation algorithm decreases the least and is always greater than capacities produced by the other two schemes.

Finally, we examine the impact of the number of subcarriers used in an adaptive WDM RoFSO system on the system capacity. In the wavelength bands starting from 1520 nm, we adopt a 1 nm spacing between adjacent wavelengths. The simulation results in clear weather are presented in Fig. 6. As we can see in Fig. 6, a system capacity increase if we adopt more subcarriers in the adaptive WDM RoFSO system. When there are 15 channels in the system, the difference between the achieved capacity of the three schemes is not much great. However, as the number of subcarriers increases, the advantage of the RoFSO power allocation scheme becomes greater.

We also run our simulations in hazy and foggy weather and presented in Figs. 7 and 8, respectively. In Fig. 7, the RoFSO power allocation algorithm achieves greater capacity with more subcarriers. System capacities increased with the number of subcarriers for all three algorithms. However, due to the simplified objective function used in the development of the water-filling algorithm, the water-filling algorithm does not achieve as much capacity as the RLT algorithm when the number of sub-carriers is 35. The RoFSO power allocation algorithm makes better use of available subcarriers to enhance system capacity and thus provide the greatest capacity. When weather conditions become worse, the system capacity become much small and the

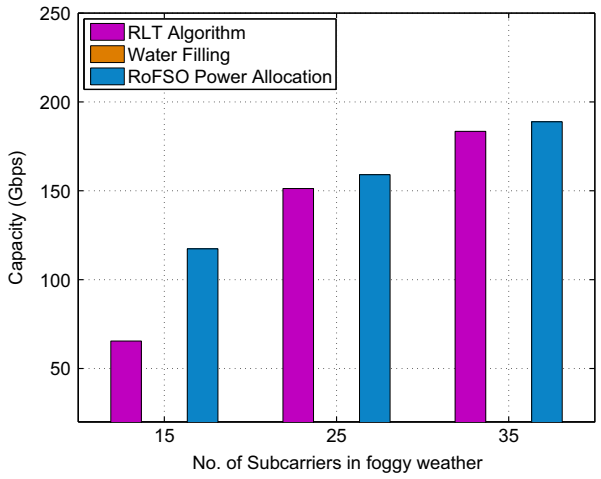

Fig. 8 System capacity versus the number of subcarriers in foggy weather.

results are shown in Fig. 8. When the weather is foggy, the capacity achieved by the water-filling algorithm is very small. But the RoFSO power allocation algorithm and the RLT algorithm can maintain system performance in foggy weather. Also when more subcarriers are utilized in the system, more system capacity can be achieved by using these two algorithms.

To conclude, the system performance in terms of capacity by using the RoFSO power allocation algorithm is the best in all situations studied here. These simulation results indicate that with proper system design, the RoFSO system can support high data rates even over long distance and under bad weather conditions.

6. Conclusions

In this paper, we investigated the problem of optical power allocation under a power budget constraint and eye safety power constraint for adaptive WDM transmission to mitigate the effect of weather turbulence, and solution algorithms are developed. For convectional transmission systems, a simple water-filling algorithm can be adopted to allocate power to different wavelengths; for WDM RoFSO systems, an RoFSO power allocation algorithm was demonstrated to achieve the greatest system capacity. It is capable of supporting high data rates even over long distance or under bad weather conditions. Utilizing multiple wavelengths in the WDM FSO system for diversity gain was also investigated in the paper.

Acknowledgements

This work was supported in part by the U.S. National Science Foundation (NSF) under Grant CNS-1320664, and through the Wireless Engineering Research and Education Center (WEREC) at Auburn University. Any opinions, findings, and conclusions or recommendations expressed in this material are those of the author(s) and do not necessarily reflect the views of the NSF.

References

[1] P. Dat, A. Bekkali, K. Kazaura, K. Wakamori, et al., Studies on characterizing the transmission of RF signals over a turbulent FSO link, Opt. Express 17 (2009) 7731–7743.
[2] H. Zhou, A. Babaei, S. Mao, P. Agrawal, Algebraic connectivity of degree constrained spanning trees for FSO networks, in: Proceedings of IEEE ICC'13, Budapest, Hungary, 2013, pp. 1–6.
[3] I.K. Son, S. Kim, S. Mao, Building robust spanning trees in free space optical networks, in: IEEE MILCOM'10, San Jose, CA, 2010, pp. 1857–1862.
[4] I.K. Son, S. Mao, Design and optimization of a tiered wireless access network, in: Proceedings of IEEE INFOCOM'10, San Diego, CA, 2010, pp. 1–9.
[5] I.-K. Son, S. Mao, S.K. Das, On the design and optimization of a free space optical access network, Opt. Switch. Netw. 11 (Part. A) (2014) 29–43. http://dx.doi.org/10.1016/j.osn.2013.08.004.
[6] I.-K. Son, S. Mao, S.K. Das, On joint topology design and load balancing in FSO networks, Opt. Switch. Netw. 11 (Part A) (2014) 92–104. http://dx.doi.org/10.1016/j.osn.2013.08.001.
[7] A. Farid, S. Hranilovic, Diversity gain and outage probability for MIMO free-space optical links with misalignment, IEEE Trans. Commun. 60 (2) (2012) 479–487.
[8] M. Karimi, M. Uysal, Novel adaptive transmission algorithms for free-space optical links, IEEE Trans. Commun. 60 (12) (2012) 3808–3815.
[9] H. Moradi, M. Falahpour, H. Refai, P. LoPresti, M. Atiquzzaman, On the capacity of hybrid FSO/RF links, in: Proceedings of IEEE GLOBECOM'10, 2010, pp. 1–5.
[10] H. Zhou, S. Mao, P. Agrawal, Optical power allocation for adaptive WDM transmission in free space optical networks, in: Proceedings of IEEE WCNC 2014, Istanbul, Turkey, 2014, pp. 2677–2682.
[11] X. Liu, Free-space optics optimization models for building sway and atmospheric interference using variable wavelength, IEEE Trans. Commun. 57 (2) (2009) 492–498.
[12] Y. Huang, S. Mao, Downlink power control for variable bit rate videos over multicell wireless networks, in: Proceedings of IEEE INFOCOM'11, 2011, pp. 2561–2569.
[13] A. Vavoulas, H. Sandalidis, D. Varoutas, Weather effects on FSO network connectivity, IEEE/OSA J. Optical Commun. Netw. 4 (10) (2012) 734–740.
[14] A. Aladeloba, M. Woolfson, A. Phillips, WDM FSO network with turbulence-accentuated interchannel crosstalk, IEEE/OSA J. Opt. Commun. Netw. 5 (6) (2013) 641–651.
[15] V. Sharma, G. Kaur, Modelling of OFDM-ODSB-FSO transmission system under different weather conditions, in: 2013 Third International Conference on Advanced Computing and Communication Technologies (ACCT), 2013, pp. 154–157.
[16] V.V. Sivakumar, D. Hu, P. Agrawal, Relay positioning for energy saving in cooperative networks, in: IEEE 45th Southeastern Symposium on System Theory, 2013, pp. 1–5.
[17] A. Johnsi, V. Saminadan, Performance of diversity combining techniques for FSO-MIMO system, in: 2013 International Conference on Communications and Signal Processing (ICCSP), 2013, pp. 479–483.
[18] H. Zhou, D. Hu, S. Mao, P. Agrawal, Joint relay selection and power allocation in cooperative FSO networks, in: Proceedings of IEEE GLOBECOM'13, Atlanta, GA, 2013, pp. 1–6.
[19] H. Zhou, S. Mao, P. Agrawal, On relay selection and power allocation in cooperative free space optical networks, Photon. Netw. Commun. J. (PNET) 29 (1) (2015) 1–11. http://dx.doi.org/10.1007/s11107-014-0465-z.
[20] M. Kashani, M. Safari, M. Uysal, Optimal relay placement and diversity analysis of relay-assisted free-space optical

communication systems, IEEE/OSA J. Opt. Commun. Netw. 5 (1) (2013) 37–47.
[21] C. Abou-Rjeily, A. Slim, Cooperative diversity for free-space optical communications: transceiver design and performance analysis, IEEE Trans. Commun. 59 (3) (2011) 658–663.
[22] I. Djordjevic, Adaptive modulation and coding for free-space optical channels, IEEE/OSA J. Opt. Commun. Netw. 2 (5) (2010) 221–229.
[23] K.-H. Kim, T. Higashino, K. Tsukamoto, S. Komaki, WDM optical power allocation method for adaptive radio on free space optics system design, in: 2011 International Topical Meeting on Microwave Photonics & 2011 Asia-Pacific Microwave Photonics Conference (MWP/APMP), Singapore, 2011, pp. 361–364.
[24] S.G. Wilson, M. Brandt-Pearce, Q. Cao, J.H. Leveque, Free-space optical MIMO transmission with Q-ary PPM, IEEE Trans. Commun. 53 (8) (2005) 1402–1412.
[25] N. Cvijetic, S. Wilson, M. Brandt-Pearce, Performance bounds for free-space optical MIMO systems with APD receivers in atmospheric turbulence, IEEE J. Sel. Areas Commun. 26 (3) (2008) 3–12.
[26] E. Ciaramella, Y. Arimoto, G. Contestabile, M. Presi, A. D'Errico, V. Guarino, M. Matsumoto, 1.28 Terabit/s (32x40 Gbit/s) WDM transmission system for free space optical communications, IEEE J. Sel. Areas Commun. 27 (9) (2009) 1639–1645.
[27] K. Kazaura, K. Wakamori, M. Matsumoto, T. Higashino, K. Tsukamoto, S. Komaki, RoFSO: a universal platform for convergence of fiber and free-space optical communication networks, in: 2009 Innovations for Digital Inclusions, ITU-T Kaleidoscope, 2009, pp. 1–8.
[28] K.-H. Kim, T. Higashino, K. Tsukamoto, et al., Statistical analysis on the optical fading in free space optical channel for RoFSO link design, in: Proceedings of SPIE 7620, Broadband Access Communication Technologies IV, 76200G, 2010, pp. 1–10.
[29] M. Safari, M. Rad, M. Uysal, Multi-hop relaying over the atmospheric poisson channel: outage analysis and optimization, IEEE Trans. Commun. 60 (3) (2012) 817–829.
[30] V. Rajakumar, M. Smadi, S. Ghosh, T. Todd, S. Hranilovic, Interference management in WLAN mesh networks using free-space optical links, J. Lightw. Technol. 26 (13) (2008) 1735–1743.

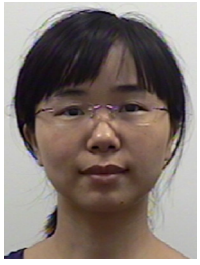

Hui Zhou received the Ph.D. in Electrical and Computer Engineering from Auburn University, Auburn, AL in 2014. She received the M.S. degree in 2009, and the B.S. degree in 2007 from Huazhong University of Science and Technology, both in Electronic and Information Engineering. Currently, she is a Software Development Engineer at Amazon Web Services, Amazon, Inc. She was a Senior DSP Software Engineer with Zhongxing Telecommunication Equipment Corporation, Shanghai, China from 2009 to 2011. Her research interests include femtocell networks and free space networks. She is a co-recipient of the IEEE International Conference on Communications (ICC) 2013 Best Paper Award.

Shiwen Mao received his Ph.D. in electrical and computer engineering from Polytechnic University, Brooklyn, NY in 2004. He was the McWane Associate Professor in the Department of Electrical and Computer Engineering from 2012 to 2015, and is the Samuel Ginn Endowed Professor and the Director of the Wireless Engineering Research and Education Center (WEREC) since 2015 at Auburn University, Auburn, AL, USA.

His research interests include wireless networks and multimedia communications. He is a Distinguished Lecturer of the IEEE Vehicular Technology Society in the Class of 2014, and the Vice Chair-Letters and Member Communications of IEEE Communications Society Multimedia Communications Technical Committee. He is on the Editorial Board of IEEE Transactions on Multimedia, IEEE Internet of Things Journal, IEEE Communications Surveys and Tutorials, and IEEE Multimedia, among others. He serves as Steering Committee Member for IEEE ICME and AdhocNets, Area TPC Chair of IEEE INFOCOM 2016 and Technical Program Vice Chair for Information Systems of IEEE INFOCOM 2015, symposium co-chairs for many conferences, including IEEE ICC, IEEE GLOBECOM, ICCCN, et al. He received the 2013 IEEE ComSoc MMTC Outstanding Leadership Award and the NSF CAREER Award in 2010. He is a co-recipient of The IEEE WCNC 2015 Best Paper Award, The IEEE ICC 2013 Best Paper Award, and The 2004 IEEE Communications Society Leonard G. Abraham Prize in the Field of Communications Systems.

Prathima Agrawal is an Emeritus professor of electrical and computer engineering, Auburn University, Auburn, Alabama. Prior to her present positions, she worked in Telcordia Technologies (formerly Bellcore), Morristown, New Jersey, and at AT&T/Lucent Bell Laboratories, Murray Hill, New Jersey. She created and served as head of the Networked Computing Research Department in Murray Hill. She is widely published and holds 51 US patents. She is a Fellow of IEEE. She received the BE and ME degrees in electrical communication engineering from the Indian Institute of Science, Bangalore, India, and the PhD degree in electrical engineering from the University of Southern California in 1977.